Construction and Building Materials 397 (2023) 132407

Contents lists available at ScienceDirect

Construction and Building Materials

journal homepage: www.elsevier.com/locate/conbuildmat

Implementing capillary pressure control measures to prevent plastic shrinkage cracking in concrete

Renier Christiaan Deysel, William Peter Boshoff *, Martha Sophia Smit

University of Pretoria, Hatfield Campus, Lynnwood Road, Pretoria, South Africa

ARTICLE INFO

Keywords:
Plastic shrinkage
Plastic shrinkage cracking
Fresh Concrete
Tensiometers
Capillary pressure
No cracking capillary pressure boundary model
Empirical model

ABSTRACT

Plastic shrinkage cracking occurs when fresh concrete is drying and restrained from deformation, which typically results in cracking. The tensile stresses causing cracking result from the negative capillary pressure that develops in the drying concrete. This study developed a model that uses live in-situ capillary pressure measurements in fresh concrete to control the capillary pressure response to prevent plastic shrinkage cracking at any reasonable evaporation rate, making it a valuable tool for preventing plastic shrinkage cracking.

1. Introduction and background

Cracks are formed in fresh concrete when restrained plastic shrinkage induces tensile stress greater than the tensile strength at the time [1,2]. This tensile strength refers to the capillary pressure and cohesion forces between the particles and not to the hydration of the cement particles in the fresh concrete. Plastic shrinkage cracks compromise aesthetics and durability and are more severe in concrete elements with large surface areas [3,4]. Concrete elements that undergo water loss through its boundary experience plastic shrinkage. Water loss may be due to evaporation from the surface or suction of the dry materials adjacent to the still plastic element [5].

Plastic shrinkage is caused by capillary pressure [6,7]. When there is water loss, there is a point at which air–water interfaces occur in capillaries in the concrete and a complicated system of menisci forms [6,8]. The complicated system of menisci causes negative capillary pressure, which can also be thought of suction. As less water is available in the concrete, the menisci radii decrease and the magnitude of capillary pressure increases, resulting in the fresh concrete mass contracting.

The capillary pressure at a specific location in concrete exposed to a constant evaporation rate is conceptually illustrated in Fig. 1. There are three stages of capillary pressure change. Stage I is directly after the concrete is placed and the capillary pressure is still zero. In this stage, all the capillaries are filled with water, and bleed water accumulates on the concrete surface. As the bleed rate decreases, and the evaporation rate remains constant, the cumulative amount of evaporated water exceeds the cumulative amount of bleed water. At the end of Stage I, all the bleed water has evaporated and the concrete surface is dry. This is referred to as drying time and here the negative capillary pressure starts to increase.

In Stage II, menisci form in the concrete. The depth of the menisci system increases as more water moves from the system and the depth of the dry concrete increases. The radii of the menisci also reduce as less water is available in the concrete. As the radii decrease, the magnitude of negative capillary pressure increases. The capillaries in the concrete contract and the plastic shrinkage occurs. The available free water can decrease until the menisci between particles can no longer be bridged. This results in air entry and the onset of plastic shrinkage cracking. Air entry is localised on the concrete surface. The period from drying time to initial set is referred to as the critical period [9].

Stage III shows the instantaneous decrease in magnitude of negative capillary pressure when air entry occurs. As the concrete surface continues to dry, other locations reach air entry and more plastic shrinkage cracks are initiated.

The capillary pressure mechanism encapsulates all the influences of climatic conditions, specimen geometry and materials composition on the cracking risk of concrete [10–13]. Kwak & Ha [14] found that drying time occurs earlier when the evaporation rate is increased, and the bleeding rate remains constant. Consequently, the magnitude of negative capillary pressure starts to increase earlier. Turcry & Loukil [15] and Combrinck & Boshoff [16] found that the onset of plastic shrinkage cracks is before or at initial set. The cracks widen and lengthen between initial and final set, whereafter the rate of crack growth decreases

* Corresponding author.
E-mail addresses: u15062890@tuks.co.za (R.C. Deysel), billy.boshoff@up.ac.za (W.P. Boshoff), phia.smit@up.ac.za (M.S. Smit).

https://doi.org/10.1016/j.conbuildmat.2023.132407
Received 9 February 2023; Received in revised form 2 July 2023; Accepted 3 July 2023
Available online 12 July 2023

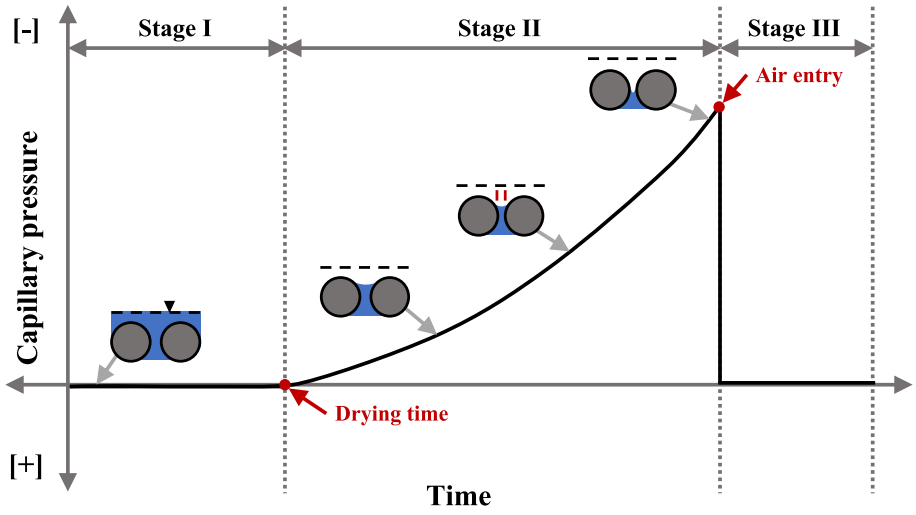

Fig. 1. Three stages of capillary pressure in fresh concrete (adapted from Slowik et al. [7]).

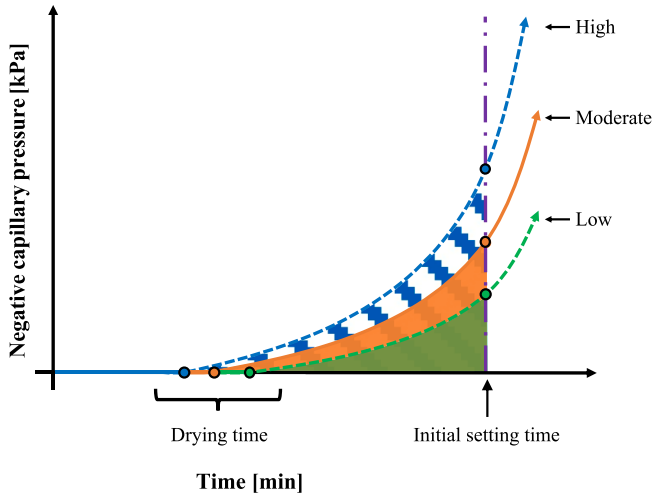

Fig. 2. Effect of capillary pressure change rate.

significantly and stabilises. Boshoff & Combinck [2] and Sayahi et al. [9] found that the severity of plastic shrinkage cracking in concrete is directly proportional to the product of the volume of evaporated water during the critical period and the initial setting time.

Plastic shrinkage cracking in fresh concrete is caused by a complex combination of parameters that can change at any moment, making this phenomenon challenging to predict. However, capillary pressure in combination with drying time and initial setting time are identified factors that dominantly influence plastic shrinkage cracking. These factors can be encapsulated/measured by the area under the capillary pressure curve between the two points in time. This pressure–time area characterises the plastic shrinkage induced by negative capillary pressure during the critical period.

Fig. 2 schematically illustrates the effect of the rate of capillary pressure change on the pressure–time area. Normally, for the same bleeding characteristics and materials composition, the drying time is earlier with higher evaporation rates, also resulting in a high rate of capillary pressure increase afterwards. It also results in a higher magnitude of negative capillary pressure at initial set. Both these effects contribute to a greater pressure–time area.

Methods and models to prevent plastic shrinkage cracking have been developed. Findings from Slowik et al. [7] and Slowik et al. [17] showed that the magnitude of negative capillary pressure can be reduced by rewetting concrete. A closed-loop rewetting as a method for curing has proved to be effective in controlling negative capillary pressure from intensifying. This method required unique instrumentation to determine the pressure threshold at which rewetting need to be implemented. Plastic shrinkage severity models proposed by Boshoff & Combrinck [2] and Sayahi et al. [9] were effective in predicting the plastic shrinkage cracking severity as a function of evaporation rate. The models were, however, only applicable to certain mould restraints and could not predict when cracking would not occur. The model proposed by Ghodousi et al. [10] for predicting plastic shrinkage cracking area could only provide a rough estimate of the plastic shrinkage cracking area in self-compacting concrete.

Capillary pressure is the driving force behind plastic shrinkage. It can be monitored in plastic concrete and controlled to prevent plastic shrinkage cracking. In this paper, a capillary pressure control measure to prevent plastic shrinkage cracking was implemented and evaluated. The potential control measure was identified, developed and refined. The input parameters for the control measure for a specific concrete mixture were determined from physical testing and the efficacy of the control measure was evaluated using different evaporation rates.

2. Model characterisation

2.1. The no cracking capillary pressure boundary model

The proposed No Cracking Capillary Pressure Boundary Model is developed from the negative capillary pressure response, the drying time and the initial setting time. The parameters are used to determine the pressure–time area under the negative capillary pressure response from the drying time to the initial setting time of the concrete. This pressure–time area is a measure of the plastic shrinkage induced by the negative capillary pressure in the mentioned timeframe.

It is postulated that to prevent plastic shrinkage cracks from forming, the pressure–time area for a curve with a high negative capillary pressure change rate, must be less than or equal to the pressure–time area of a capillary pressure response curve that does not result in cracking. For the pressure–time areas to be less than or equal, a no cracking capillary pressure boundary must be determined. The negative capillary pressure of the high negative capillary pressure change rate concrete must be maintained within this boundary. This boundary can be applied by determining a critical pressure limit on the high negative capillary pressure response. The larger the negative capillary pressure change rate, the lower the no cracking capillary pressure boundary will be to ensure that the pressure–time area remains less than or equal to the

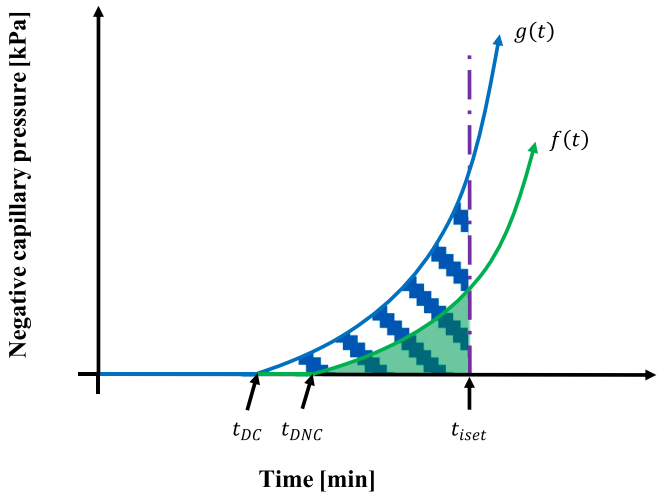

Fig. 3. The schematic of the negative capillary pressure response and pressure–time areas of $g(t)$ that will have plastic shrinkage cracking and $f(t)$ that will have no plastic shrinkage cracking.

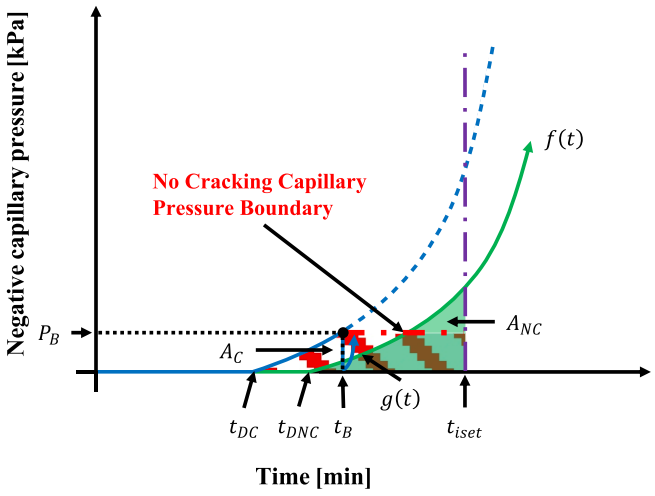

Fig. 4. The schematic of the negative capillary pressure responses of $g(t)$ and $f(t)$ with equal pressure–time areas after applying the model concept.

pressure–time area of the capillary pressure response curve that does not result in cracking.

The model concept can be explained with the schematic illustrations in Fig. 3 and Fig. 4. Fig. 3 shows two negative capillary pressure response curves at different change rates that passes the initial setting time of the concrete at t_{iset}. The negative capillary pressure response of $g(t)$ is greater than that of $f(t)$. The upper curve, $g(t)$, is the negative capillary pressure response curve of fresh concrete that will form plastic shrinkage cracks. The second curve, $f(t)$, is the negative capillary pressure response of the same fresh concrete that will just not form plastic shrinkage cracks. If the negative capillary pressure response of $f(t)$ were any higher, plastic shrinkage cracking would occur.

Fig. 3 also shows the pressure–time area under the negative capillary pressure response between the drying time and the initial set for $g(t)$ and $f(t)$. The area under $g(t)$ is greater than the area under the no crack curve $f(t)$.

By applying the No Cracking Capillary Pressure Boundary Model, it is proposed that for no plastic shrinkage cracks to occur on the concrete of $g(t)$, the pressure–time area under $g(t)$ must be equal or less to the pressure–time area under the no crack curve $f(t)$. For the area under $g(t)$ to be equal to the area under $f(t)$, a no cracking capillary pressure boundary must be applied at a specific time to the negative capillary pressure response curve $g(t)$. The capillary pressure of the concrete needs to be maintained under the boundary. Fig. 4 shows the two negative capillary pressure response curves, $g(t)$ and $f(t)$, where no cracking capillary pressure boundary is applied to curve $g(t)$. The figure illustrates that for the area, A_S, to be equal to the area, A_{NC}, a no cracking capillary pressure boundary must be applied to curve $g(t)$ at a specific time, t_B. The no cracking capillary pressure boundary marks the critical pressure limit, P_B, for area A_C, for curve $g(t)$ to be maintain under.

Therefore, the critical pressure limit, P_B and corresponding time, t_B need to be determined to apply the no cracking capillary pressure boundary to a negative capillary pressure response. The critical pressure limit and corresponding time can be derived from Fig. 4 by considering:

$$A_{NC} = A_C \tag{1}$$

where A_{NC} is the area of the negative capillary pressure response curve of concrete that will not form plastic shrinkage cracks [kPa·min] and A_C is the area of the negative capillary pressure response curve of concrete that will form plastic shrinkage cracks [kPa·min].

The pressure–time area of A_{NC} and A_C can be found by integrating the required regions:

$$\int_{t_{DNC}}^{t_{iset}} f(t)dt = \int_{t_{DC}}^{t_B} g(t)dt + P_B \bullet (t_{iset} - t_B) \tag{2}$$

where t_{iset} is the initial setting time [min], t_{DNC} the drying time of the no crack negative capillary pressure response curve [min] and t_{DC} drying time of the negative capillary pressure response curve of the concrete that will form plastic shrinkage cracks [min]. Furthermore, t_B is the time correlating to the critical pressure limit [min] and P_B the critical pressure limit [kPa].

The expression for the negative capillary pressure response of $f(t)$ and $g(t)$ is unknown, making it challenging to calculate the area under the negative capillary pressure response with Eq. (2). Therefore, the Trapezoidal rule is used to calculate the areas under the negative capillary pressure response curves. By substituting the Trapezoidal rule into the previous expression, the no cracking capillary pressure boundary equation is found.

$$\frac{h}{2}\left[f(t_{DNC}) + 2\sum_{a=1}^{n-1} f(t_{1_a}) + f(t_{iset})\right] = \frac{h}{2}\left[g(t_{DC}) + 2\sum_{b=1}^{m-1} g(t_{2_b}) + g(t_B)\right] + P_B \bullet (t_{iset} - t_B),$$

$$a = 1, 2, \cdots, n-2, n-1$$

$$(where\ t_{1_0} = t_{DNC}\ and\ t_{1_n} = t_{iset})$$

$$and \tag{3}$$

$$b = 1, 2, \cdots, m-2, m-1$$

$$(where\ t_{2_0} = t_{DC}\ and\ t_{2_m} = t_B)$$

Table 1
The concrete mix design and properties.

Water [kg/m^3]	CEM I 52.5 R [kg/m^3]	13.2 mm Dolomite crusher stone [kg/m^3]	Dolomite crusher sand [kg/m^3]	Slump [mm]	28-day Compressive strength [MPa]	Initial setting time [min]	Final setting time [min]
220	440	453	1359	10	49.5 (3.11)	283	430

where h is the time intervals [min] used to determine the pressure–time areas.

By simplifying Eq. (3), the no cracking capillary pressure boundary equation can be expressed as:

$$T_{RNC} = T_{RC} + P_B \bullet (t_{iset} - t_B) \quad (4)$$

Where T_{RNC} is the Trapezoidal rule estimate for the area under $f(t)$ [kPa·min] and T_{RC} the Trapezoidal rule estimate for the area under $g(t)$ between the drying time and the time when the no cracking capillary pressure boundary is applied [kPa·min].

Hence, the No Cracking Capillary Pressure Boundary Model is found. By maintaining the negative capillary pressure response of $g(t)$ below the no cracking capillary pressure boundary which marks P_B, to obtain the same pressure–time area as that of the no crack capillary pressure response $f(t)$, plastic shrinkage cracking could be prevented.

2.2. The no cracking capillary pressure boundary model determination

To apply the proposed model with live or previous capillary pressure measurements, Eq. (3) is used to calculate the critical pressure limit and the time at which this limit is reached. Eq. (3) sets the pressure–time area of the no crack curve equal to the pressure–time area of the curve where plastic shrinkage needs to be prevented. Only three model parameters are required for this equation:

1. the area under the no crack negative capillary pressure response for the relevant concrete
2. the drying time of the current negative capillary pressure response
3. the initial setting time of the relevant concrete

The critical pressure limit can then be determined by adding the negative capillary pressure measurements and the corresponding time after the current drying time into Eq. (3). The capillary pressure measurements and corresponding time is added at 60-second intervals until the pressure–time area is equal to the area T_{RNC}. The 60-second intervals were decided on to provide sufficient accuracy to determine the pressure–time area and notice any sudden changes in the negative capillary pressure change rate. When the critical pressure limit is reached, the negative capillary pressure response will need to be reduced by rewetting the concrete. The no cracking capillary pressure boundary marks the critical pressure limit and is applied when the pressure limit is reached. The negative capillary pressure response is reduced by rewetting the concrete surface each time the no cracking capillary pressure boundary is reached.

The benefit of the proposed empirical model is that the model only requires three parameters and can be applied in real-time and with previous capillary pressure measurements in fresh concrete to help prevent plastic shrinkage cracking.

3. Experimental framework

3.1. Experimental outline

The experimental work consisted of two testing phases namely the plastic shrinkage cracking characterisation and model verification phase. The phases assist in evaluating the proposed No Cracking Capillary Pressure Boundary Model. In the plastic shrinkage cracking characterisation phase, the concrete was tested at six evaporation rates to determine the model parameters needed for testing the model. In the model verification phase, the concrete was tested in three evaporation rates to evaluate whether the model can be used to reduce plastic shrinkage cracking. The capillary pressure, evaporation rate, and plastic shrinkage cracks were measured during each phase.

Table 2
The chemical compounds of CEM I 52.5 R [% by mass, ignited basis], Afrisam [22].

SiO_2	CaO	Al_2O_3	Fe_2O_3	MgO
20.79	65.05	4.64	2.69	1.73

3.2. Materials and mixture proportions

A low bleed concrete mix was used for the experimental work which consisted of 75 % fine aggregate and 25 % coarse aggregate. Table 1 shows the material constituents and mixture proportions. The slump [18], compressive strength [19] and setting times [20] of the concrete are also shown in the table. The standard deviation for the 28-day compressive strength is provided in the table in brackets. Time zero for the setting time was when the water made contact with the cement. The concrete has a water/cement ratio of 0.5 and bleeding capacity of 1.18 kg/m^2 [21].

The CEM I 52.5 R used in the mix design has a specific surface area and particle size range of 609 m^2/kg and 0.3 – 350 μm, respectively. The chemical composition of the cement is provided in Table 2.

In both testing phases, the concrete was cast into three evaporation moulds and three plastic shrinkage cracking moulds. The evaporation moulds were cylindrical PVC moulds with a diameter of 110 mm and a height of 100 mm. Fig. 5 shows the plastic shrinkage cracking mould used as well as the dimensions of the mould. The figure also shows where the tensiometers were placed within the concrete specimens. The plastic shrinkage cracking mould was adapted in two ways, initially by Combrinck [23] from the original ASTM C 1579 [24] mould design and thereafter by adding four vertical triangular prisms taken from a design by Combrinck et al. [25], with two at each endpoint.

The experimental work used a tensiometer setup, as illustrated in Fig. 6. The setup featured an upwards facing tensiometer, situated in 32 mm from the surface of the concrete and held in place with a specially designed three-dimensional printed pedestal. The purpose of the pedestal was to maintain the tensiometer at the desired height and position in the concrete specimens after vibrating the concrete, as shown in the figure.

The constituents and moulds were placed in a temperature-controlled room (set at an air temperature of 24 ± 1 °C) 24 h before testing. The mixing procedure for the concrete started by wetting the pan mixer. The dry constituents were then added to the mixer and mixed for 60 s. Thereafter the water was added, and the concrete was mixed for 2 min, which added up to a total mixing time of 3 min.

3.3. Experimental setup

The evaporation rates needed for the different tests in each phase were created using a:

- Climate Chamber (high evaporation rates with controllable wind speeds) – one evaporation rate in the plastic shrinkage cracking

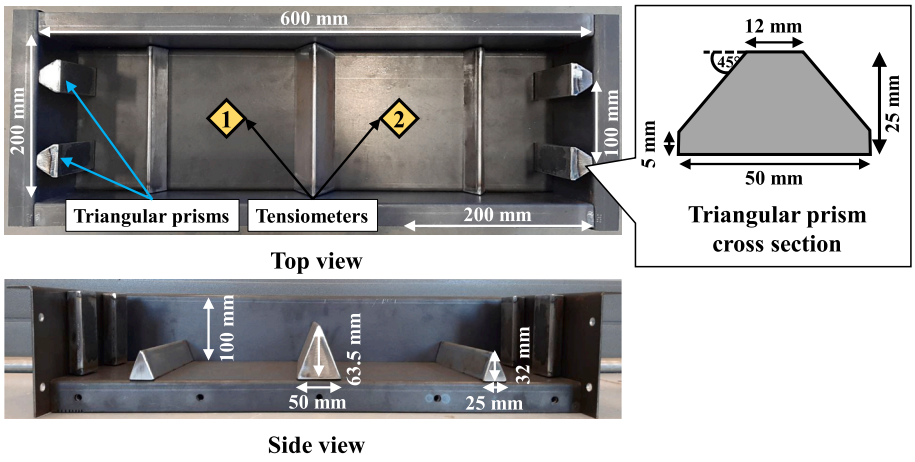

Fig. 5. Plastic shrinkage cracking mould with dimensions and tensiometer placement.

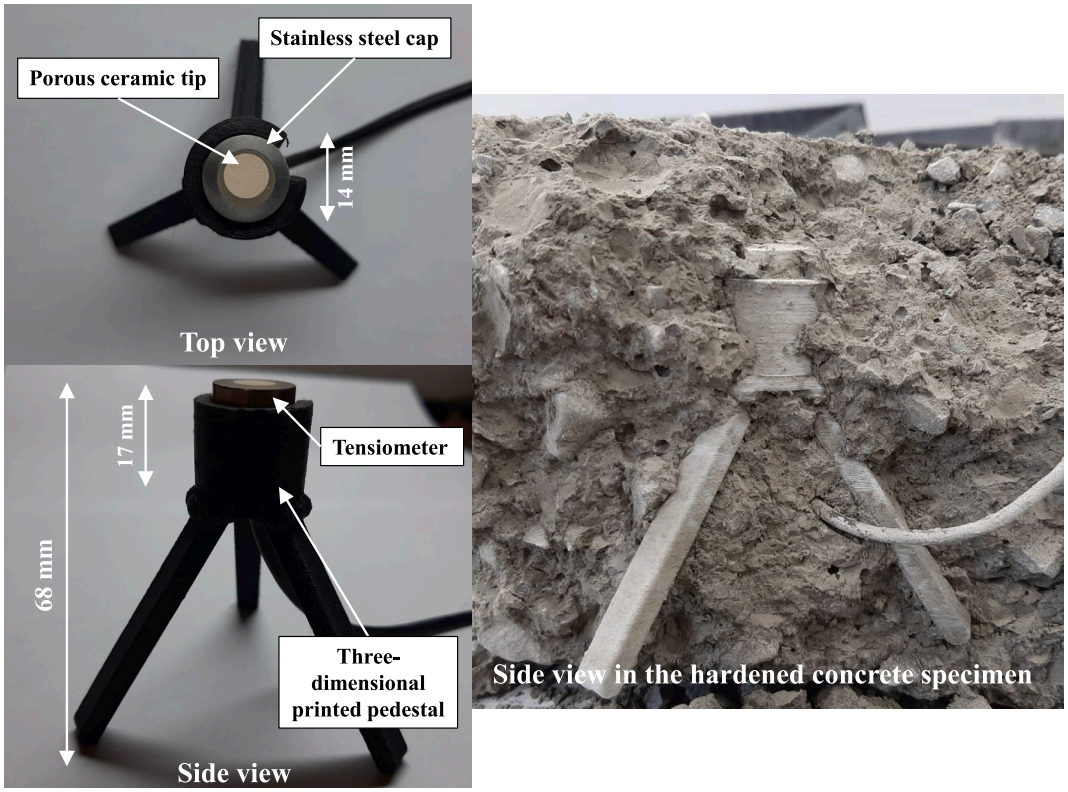

Fig. 6. Tensiometer setup with dimensions.

characterisation phase and the evaporation rates in the model verification phase.

- Mild Environmental Room (mild evaporation rates) – four evaporation rates in the plastic shrinkage cracking characterisation phase.
- High Humidity Room (low evaporation rates) – only one evaporation rate for the plastic shrinkage cracking characterisation phase.

The climate chamber was set at the desired climatic conditions (temperature, wind, humidity) 2 h before the test, whereas the climatic-controlled rooms were set 48 h before each test (only temperature and humidity, no wind).

The capillary pressure in the fresh concrete was measured with tensiometers that can measure the direct negative capillary pressure [26,27]. Two types of tensiometers were used in the experimental setup, each consisting of a porous ceramic tip, a pressure gauge, and a stainless-steel cap. The first type had a 300 kPa porous ceramic tip and a 700 kPa pressure gauge with a maximum linearity of ± 0.5% Full Scale (FS) and a maximum pressure hysteresis of ± 0.15% FS. The second type had a 1500 kPa ceramic tip and a 1200 kPa pressure gauge with a maximum linearity of ± 0.15% FS and a maximum pressure hysteresis of ± 0.15% FS.

Before each test, the tensiometers were saturated for 48 h. After saturating the tensiometers, the sensors were calibrated (all tensiometers achieved an R^2-value > 0.95) and stored in a bottle containing deaerated water until use. When embedding the tensiometers at the desired position in the concrete, the sensors were consolidated within 60 s to prevent early cavitation. Deysel [28] provides an in-depth discussion on the tensiometer design and setup and the saturation and calibration procedures utilised. The tensiometers were connected to a Campbell Scientific CR 1000X Series data acquisition system. The

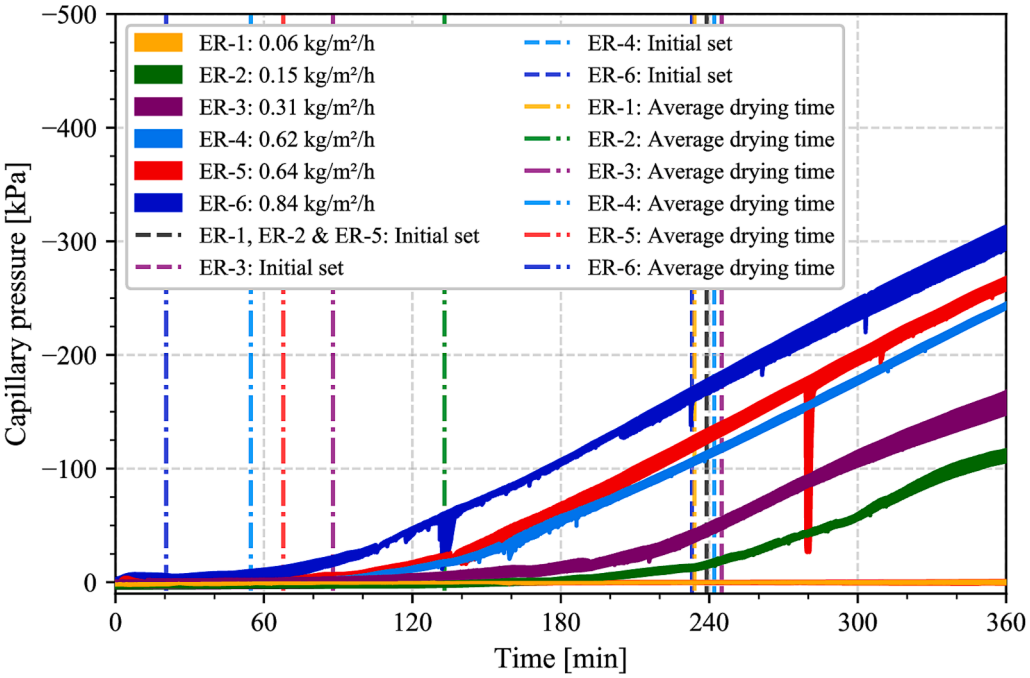

Fig. 7. The negative capillary pressure response envelopes at the six evaporation rates.

readings of the tensiometers were logged at a rate of 1 Hz for the duration of the tests. As illustrated in Fig. 5, two tensiometers (one 700 kPa tensiometer and one 1200 kPa tensiometer) were embedded at a depth of 32 mm in each plastic shrinkage cracking specimen at third points (spaced at 200 mm).

The concrete was cast in the different moulds by initially filling the moulds halfway and vibrated for 60 s. Tensiometers were placed in the plastic shrinkage cracking moulds at the desired position and depth. The moulds were filled with concrete to the 100 mm height and vibrated for another 60 s. The total duration of the vibration of the concrete adds up to 2 min. The concrete surface was finished with a steel trowel for a smooth surface finish.

The evaporation of the concrete was measured by weighing three moulds filled with fresh concrete. The specimens were measured on a Jadever JWA 30 K scale, which has a range of 30 kg and a resolution of 0.001 kg. The specimens were measured before starting the test and thereafter in intervals of 20 min for the test duration. It should be noted that 0.001 kg resolution means that evaporation rates lower than 0.11 kg/m^2/h (calculated dividing the scales resolution by the specimen surface area per hour) are likely to be an approximation of the actual evaporation rate.

The crack widths were measured every 20 min from the start of the test with a crack width card. Cracks were measured at the centre of the plastic shrinkage cracking specimens. The crack width card could measure crack widths from 0.05 to 10 mm.

In all the tests conducted in the two testing phases, the plastics shrinkage cracking and evaporation specimens were placed parallel to the wind direction in the climatic rooms and mobile climate chamber. Time zero for all of the tests began once the desired evaporation rate was reached. The concrete was then exposed to the evaporation rate for 6 h.

In the plastic shrinkage characterisation phase, the concrete was exposed to six evaporation rates (which ranged between 0.06 and 0.84 kg/m^2/h) to determine the model parameters. While the concrete was exposed to the evaporation rates, the capillary pressure, evaporation rate and cracks width were measured. In addition, capillary pressure measurements were used to determine the drying time.

In the model verification phase, the concrete was exposed to three evaporation rates (ranging between 0.35 and 0.86 kg/m^2/h). A spreadsheet was created for the empirical model, and the model parameters were added. The capillary pressure was monitored, and once the drying time (point in time where the capillary pressure $\geq$ 0 kPa) was reached, the capillary pressure measurements were added every 60 s. As the measurements were added, the spreadsheets calculated the pressure–time area until the critical pressure limit was determined. When the limit was determined, the no cracking capillary pressure boundary was applied, and the concrete surface was rewetted with water. The plastic shrinkage cracking specimens were rewetted each time the boundary was reached. A spray bottle was used to rewet each specimen. The rewetting procedure consisted of lightly drizzling (to evenly distribute the water over the surface) the water on the surface of the specimens until the pressure drop occurred. In tests conducted in this phase, the capillary pressure, evaporation rate, cracks width and water added to the specimens were measured. This process of determining whether water needs to be added and even the adding of the water can be easily automated.

Table 3
Average capillary pressures of the concrete at the different evaporation rates.

Conditions	ER-1	ER-2	ER-3	ER-4	ER-5	ER-6
Capillary pressure before cracking, kPa	–	–	−14.1	−12.5	−12.9	−14.3
Capillary pressure at the onset of cracking, kPa	–	–	−22.6	−20.1	−21.8	−24.5
Capillary pressure at the initial setting time, kPa	0.231	−18.1	−52.2	−114	−106	−158
Drying time, min	234	133	87.9	54.7	67.8	20.5

4. Results and discussions

4.1. Plastic shrinkage cracking characterisation

The negative capillary pressure envelopes overtime for the concrete at varying evaporation rates are shown in Fig. 7. Each envelope was obtained either using the highest and lowest negative capillary pressure readings or the most representable curves for each evaporation rate. The

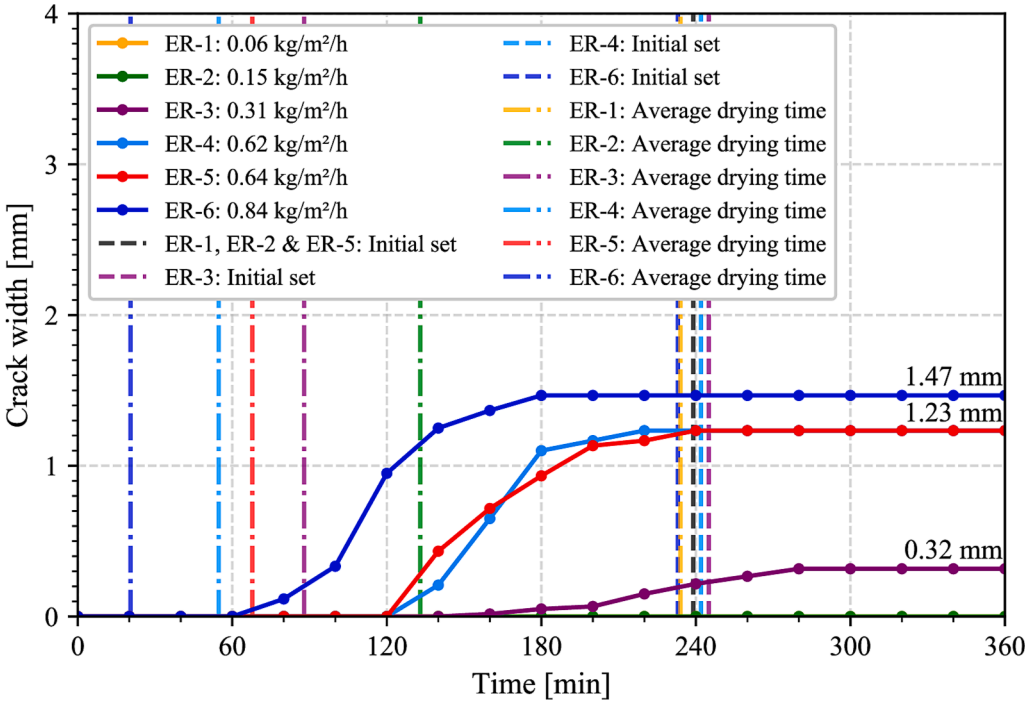

Fig. 8. The average crack width at different evaporation rates.

setting times for each evaporation rate is also shown in the figure.

The figure clearly shows that as the evaporation rate increases relative to ER-1: 0.06 kg/m^2/h, the negative capillary pressure increases which is consistent with Slowik et al. [17]. A reason for this is that the higher evaporation rates decreases the menisci radii between solid particles at a higher rate, causing the negative capillary pressure to increase substantially.

According to the findings from Holt & Leivo [29] and Slowik et al. [7], a drop in pressure in the negative capillary pressure occurs either with air entry into the concrete or by rewetting the concrete surface. The pressure drops were found to occur between the plastic shrinkage cracking onset and crack width stabilisation. Some of the pressure drops can also be seen in the negative capillary pressure envelopes of ER-4, ER-5 and ER-6. Therefore, the pressure drops might be due to sudden water movement or air entry within the concrete as a crack forms.

Table 3 shows the capillary pressure at the time of the specific events of crack formation and initial set for the different evaporation rates. The specific events of crack formation in the table include the capillary pressure just before plastic shrinkage cracking occurred (capillary pressure before cracking) and just after the onset of plastic shrinkage cracking occurred (capillary pressure at the onset of cracking). It should be noted that crack measurements were measured at 20-minute intervals, which means that the critical capillary pressure at which plastic shrinkage cracks form could be lower than the recorded capillary pressure values.

The specimens exposed to ER-1: 0.05 kg/m^2/h and ER–2: 0.15 kg/m^2/h had no plastic shrinkage cracking, while the concrete exposed to ER-2 did show an increase of negative capillary pressure, as seen in Fig. 7. Therefore, confirming that a negative capillary pressure can exist if there is no plastic shrinkage cracking. An interesting finding shown in the figure is that at the low evaporation rate ER-2, negative capillary pressure response obtained an S-type curvature. A possible cause is that the concrete surface has densified to a point where low evaporation does not affect negative capillary pressure response in the concrete and that the response is now due to water loss due to cement hydration within the concrete.

Another phenomenon shown in the table is that the capillary pressure before plastic shrinkage cracking and the capillary pressure at the onset of plastic shrinkage cracking at different evaporation rates occurred roughly at the same capillary pressure values. Before any plastic shrinkage cracks formed, the capillary pressure values were between −14.3 and −12.5 kPa in evaporation rates between ER-3: 0.31 kg/m^2/h to ER-6: 0.84 kg/m^2/h. At the onset of the plastic shrinkage cracking, the capillary pressure occurred between −24.5 and −20.1 kPa for evaporation rates between 0.31 and 0.84 kg/m^2/h (ER-3 to ER-6). It can be argued that by maintaining the negative capillary pressure response for the concrete below negative 12.5 kPa, no plastic shrinkage cracks will form. This confirms the conclusion made by Slowik et al. [17] that there exists a critical capillary pressure. As expected, the negative capillary pressure values at the initial setting time will increase with the increase in the evaporation rate.

The results show that as the evaporation rate increased, the drying time occurred sooner. The drying times found at the different evaporation rates confirm the findings from Kwak & Ha [14] on concrete drying time.

The negative capillary pressure in ER-2 for this concrete mix is used in the empirical model as the no cracking negative capillary pressure curve.

The plastic shrinkage crack growth at the various evaporation rates is illustrated in Fig. 8. Each line represents the average crack growth in that evaporation rate. Fig. 8 clearly shows that as the evaporation rate increased, the crack width increased, which corresponds to the literature [2,9]. Higher evaporation rates induce higher tensile stresses on the surface of the concrete, resulting in earlier plastic shrinkage cracking.

From Fig. 8 and Table 3 it is clear that an increase of the negative capillary pressure results in an increased cracks width. The higher negative capillary pressure will result in high tensile strains forming in the concrete and more severe plastic shrinkage cracking. The cracks initiated when the negative capillary pressure passed a critical capillary pressure, which corresponds to the conclusion Slowik et al. [17] made. In addition, the findings show that the plastic shrinkage cracks continued to grow until the initial setting time, and stabilise towards

Table 4
The previous capillary pressure results and model results for the concrete.

Conditions	ER-1	ER-2	ER-3	ER-4	ER-5	ER-6
Actual evaporation rate, kg/m^2/h	0.06	0.15	0.31	0.62	0.64	0.84
Initial setting time, min	239	239	245	242	239	233
Average capillary pressure response area, kPa·min	−2.570	−634.8	−2317	−7335	−8130	−12140
Average calculated critical pressure limit, kPa	–	–	−3.81	−3.20	−3.29	−2.95
Average crack width, mm	0	0	0.32	1.23	1.23	1.47

final set, which correlates with Combrinck & Boshoff [16].

The plastic shrinkage crack onset time at evaporation rates ER-4: 0.62 kg/m^2/h and ER-5: 0.64 kg/m^2/h coincided. It is due to the ER-4 and ER-5 having similar evaporation rates. Fig. 8 shows that between 120 and 240 min, the crack growth of ER-4 and ER-5 had different widths over time but obtained the same stabilisation crack width after 240 min. The reason for this might be due to the difference in climatic conditions although both obtained the similar evaporation rates. Furthermore, the findings show that reducing the evaporation rate from ER–4: 0.62 kg/m^2/h to ER–3: 0.31 kg/m^2/h, resulted in delaying the crack onset and the crack stabilisation times. In all of the evaporation rates, plastic shrinkage cracking initiated before the concrete reached the initial setting time.

The average crack widths of the concrete for each evaporation rate increased as the evaporation rate increased. When comparing the crack widths at stabilisation in ER-3: 0.31 kg/m^2/h with ER-4: 0.62 kg/m^2/h, the crack width of ER-4 increased by 2.84 times the crack width of ER-3. This emphasises how the evaporation rate affects the crack width of plastic shrinkage cracks.

4.2. Model verification

4.2.1. Previous capillary pressure measurement tests

Table 4 provides the three model parameters and the average crack width of the concrete for the six evaporation rates. The average capillary pressure response area and average critical pressure limit that were calculated from the six capillary pressure measurements are also shown in the table. The findings show that the negative capillary pressure response area increased as the evaporation increased. As the negative capillary pressure response area increased after the no crack negative capillary pressure response area (ER-2), the average crack width in the concrete also increased. The reason for the occurrence is that the higher the evaporation rate, the higher the negative capillary pressure response in the concrete. The higher the amount of plastic shrinkage within the concrete, the more severe the plastic shrinkage cracking on the concrete surface will be when the concrete is restrained.

The calculated critical pressure limit increased as the capillary pressure response area decreased. When comparing the critical pressure limit of ER-4: 0.62 kg/m^2/h with ER-5: 0.64 kg/m^2/h. It can be seen that ER-5 had a higher evaporation rate, but a lower average calculated critical pressure limit than that of ER-4. This might have due to ER-5 having some negative capillary pressure responses that were lower than that of ER-4, which resulted in the model calculating a lower critical pressure limit. The model was developed to calculate a higher critical pressure limit as the capillary pressure change rate decreased (increase in the evaporation rate) and vice versa. Therefore, it can be seen that the critical pressure limit equation performed correctly in determining the critical pressure limit required to apply the no cracking capillary pressure boundary.

Fig. 9 shows the regression line for plotting the negative capillary pressure response area against the evaporation rate. The figure shows that the evaporation rate increases as the negative capillary pressure response area increases. A strong linear relationship can be seen between the negative capillary pressure response area and the evaporation rate.

At the same time, Fig. 10 shows the regression line for plotting the average crack width and no cracking capillary pressure boundary (that will have to be applied) against the negative capillary pressure response.

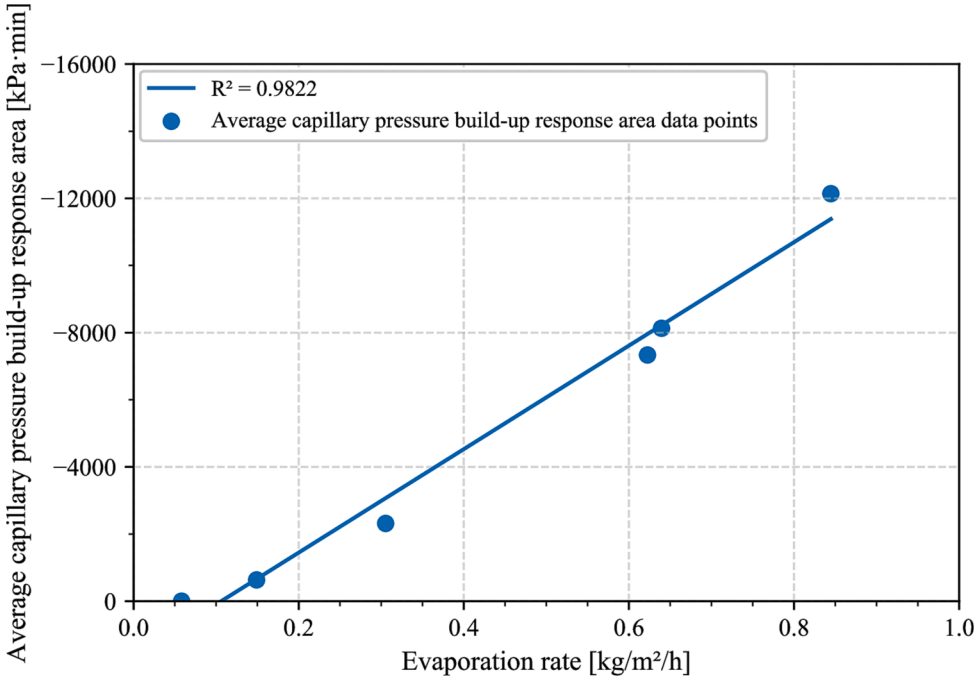

Fig. 9. The average negative capillary pressure response area versus the evaporation rate.

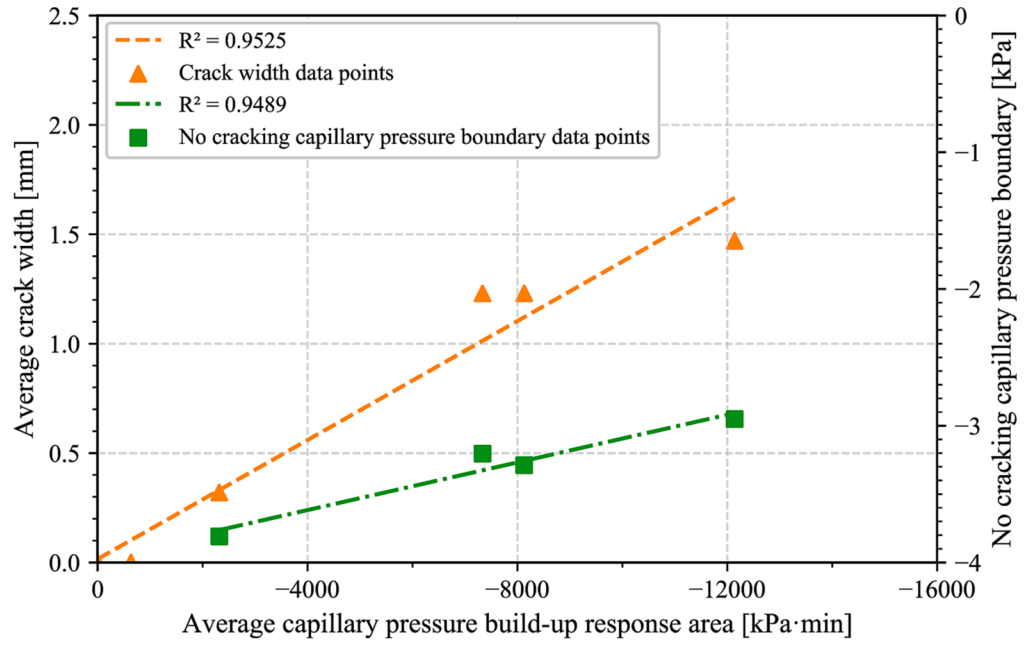

Fig. 10. Average crack width and no cracking capillary pressure boundary versus the negative capillary pressure response area.

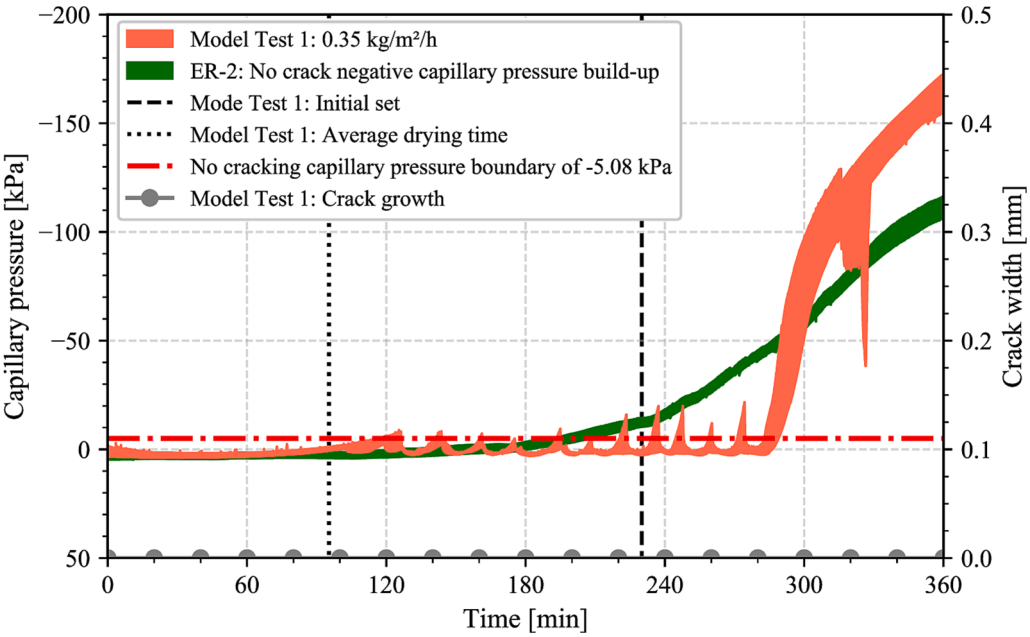

Fig. 11. Negative capillary pressure response envelope and crack width for Model Test 1.

The R^2-value of 0.953 shows a strong correlation between the average crack width and the negative capillary pressure response area of the concrete. A similar correlation between the no cracking capillary pressure boundary and the negative capillary pressure response area is seen. As the negative capillary pressure response area of the concrete increase, the average crack width increases while the no cracking capillary pressure boundary decreases.

Given the strong correlation between the plotted parameters, it can be argued that the two graphs can be utilised to predict the average plastic shrinkage crack width and the necessary boundary for preventing these cracks, using only the measured evaporation rate of the concrete.

4.2.2. Live in-situ capillary pressure measurement test

Figs. 11–13 show the negative capillary pressure response envelopes found by applying the model at three distinctive evaporation rates. The graph shows the capillary pressure and cracks width measurements over time. The concrete was only sprayed with water for up to 280 min to observe the negative capillary pressure behaviour of the concrete after the added water.

The figures show that as the evaporation rate increased, the no cracking capillary pressure boundary increased from −5.08 to −2.96 kPa. This confirms that the model correctly calculated the critical pressure limits as the evaporation rate increased. It can also be seen that all the calculated critical pressure limits were lower than the critical capillary pressures between −14.3 and −12.5 kPa from Table 3.

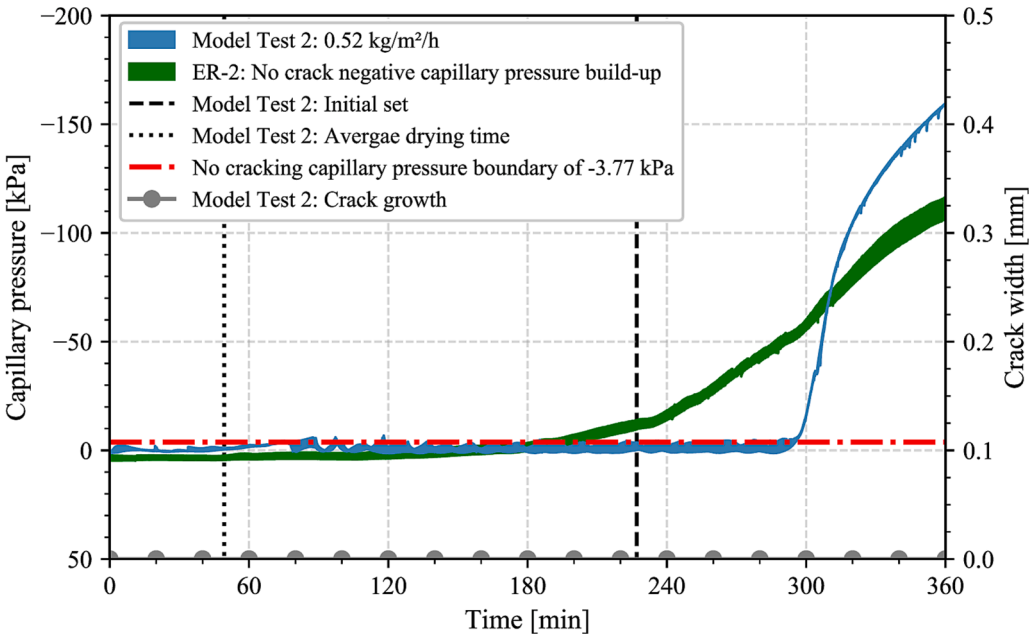

Fig. 12. Negative capillary pressure response envelope and crack width for Model Test 2.

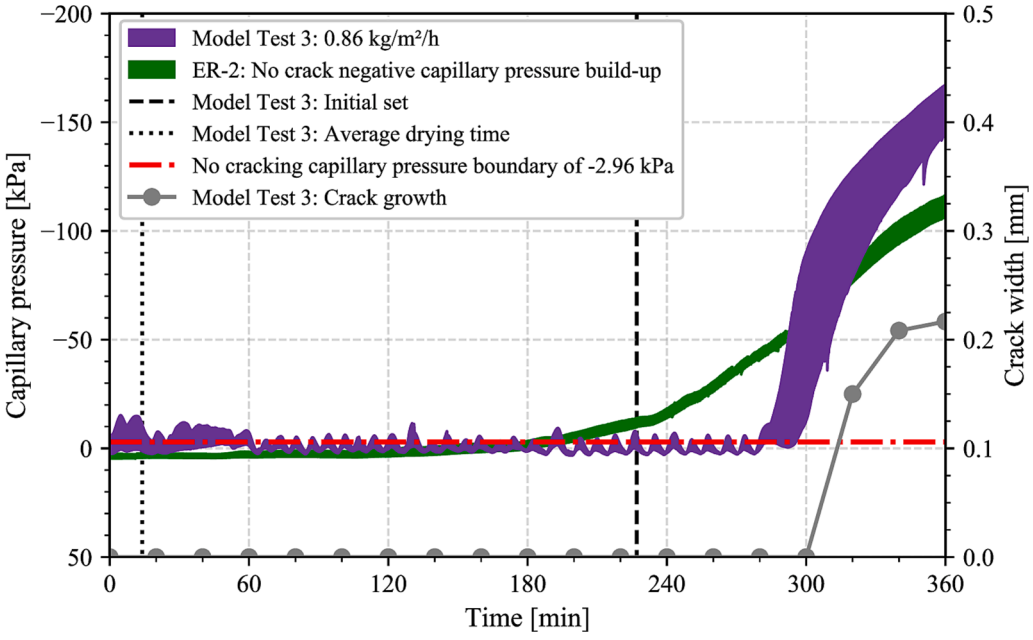

Fig. 13. Negative capillary pressure response envelope and crack width for Model Test 3.

All the Model Tests show that no plastic shrinkage cracks formed for the time that water was added when the no cracking capillary pressure boundary was reached. However, when no water was added after 280 min, only the specimens of Model Test 3 started forming plastic shrinkage cracks.

When comparing the three Model Test graphs with each other, all of the model tests followed more or less the same capillary pressure response curve when no water was added, and only the Model Test 3: 0.86 kg/m^2/h cracked. The figure shows that at the start of the Model Test 3, the capillary pressure passed the no cracking capillary pressure boundary, and water had to be added to reduce the negative capillary pressure in the concrete. The sudden negative capillary pressure response in the concrete could have damaged the concrete from the start of the test.

The graphs also show that after 280 min, the negative capillary pressure response in the concrete had similar rates. A plausible reason for the negative capillary pressure response being the same in all the Model Tests after 280 min is that at that point, the negative capillary pressure response was no longer dependent on the evaporation rate and only dependent on the hydration of the cement. Indicating that plastic shrinkage cracking is not dependent on the capillary pressure in the concrete after a certain point in time. Another reason might be that the concrete surface and the inner concrete in which the sensors were placed are now at different stages.

The findings confirmed that by using the No Cracking Capillary Pressure Boundary Model, plastic shrinkage cracking could be prevented by maintaining the negative capillary pressure response below the no cracking capillary pressure boundary.

5. Conclusions

The plastic shrinkage cracking characteristics of a concrete mixture were studied, focusing on the capillary pressure mechanism in fresh concrete. The study developed a model that uses live in-situ capillary pressure measurements in fresh concrete to control the capillary pressure response to prevent plastic shrinkage cracking at any evaporation rate. The following conclusions are drawn based on the finding obtained throughout the study:

- The plastic shrinkage and plastic shrinkage cracking characteristics of the concrete shows that as the evaporation rate increases, the negative capillary pressure change rate and plastic shrinkage crack width increases.
- The negative capillary pressure will not build up before initial set is reached, as long as the evaporation rate remains below approximately 0.1 kg/m^2/h.
- A negative capillary pressure response curve exists for the concrete tested where no plastic shrinkage cracking will occur.
- The Model Tests findings showed that the No Cracking Capillary Pressure Model calculated a critical pressure limit relevant to the concrete mixture and evaporation rate. In addition, it was seen that the calculated critical pressure limits were lower than the range of critical capillary pressures where cracking occurred.
- A model known as the No Cracking Capillary Pressure Boundary Model was proposed. The model helped prevent and reduce plastic shrinkage cracking in the concrete. After calibrating the model, by maintaining the boundary for the duration of the concrete exposed to an evaporation rate, the model can effectively aid in preventing plastic shrinkage cracking in fresh concrete.

CRediT authorship contribution statement

Renier Christiaan Deysel: Methodology, Formal analysis, Investigation, Writing – original draft. **William Peter Boshoff:** Conceptualization, Methodology, Resources, Writing – review & editing, Supervision. **Martha Sophia Smit:** Conceptualization, Methodology, Resources, Writing – review & editing, Supervision.

Declaration of Competing Interest

The authors declare that they have no known competing financial interests or personal relationships that could have appeared to influence the work reported in this paper.

Data availability

Data will be made available on request.

Acknowledgements

The author is grateful for the testing facilities and scholarship provided by the University of Pretoria.

References

[1] A.M. Neville, Properties of Concrete, 5th ed., Pearson Education Limited, Harlow, 2011.
[2] W.P. Boshoff, R. Combrinck, Modelling the severity of plastic shrinkage cracking in concrete, Cem. Concr. Res. 48 (2013) 34–39, https://doi.org/10.1016/j.cemconres.2013.02.003.
[3] M.B. Otieno, M.G. Alexander, H.-D. Beushausen, Corrosion in cracked and uncracked concrete – influence of crack width, concrete quality and crack reopening, Mag. Concr. Res. 62 (2010) 393–404, https://doi.org/10.1680/macr.2010.62.6.393.
[4] C. Qi, Quantitative assessment of plastic shrinkage cracking and its impact on the corrosion of steel reinforcement, Master's Dissertation, Purdue University, 2003.
[5] L. L'Hermite, Volume changes of concrete. 4th International Symposium on the Chemistry of Cement, National Bureau of Standards, Washington, 1960.
[6] F.H. Wittmann, On the action of capillary pressure in fresh concrete, Cem. Concr. Res. 6 (1) (1976) 49–56.
[7] V. Slowik, M. Schmidt, R. Fritzsch, Capillary pressure in fresh cement-based materials and identification of the air entry value, Cem. Concr. Compos. 30 (2008) 557–565, https://doi.org/10.1016/j.cemconcomp.2008.03.002.
[8] T.A.V. Gaspar, The tensile behaviour of three unsaturated soils subjected to the Brazilian Disc Test, University of Pretoria, 2017. Master's dissertation.
[9] F. Sayahi, M. Emborg, H. Hedlund, A. Cwirzen, M. Stelmarczyk, The severity of plastic shrinkage cracking in concrete: A new model, Mag. Concr. Res. 73 (2021) 315–324, https://doi.org/10.1680/jmacr.19.00279.
[10] P. Ghoddousi, A.M. Abbasi, E. Shahrokhinasab, M. Abedin, Prediction of Plastic Shrinkage Cracking of Self-Compacting Concrete, Adv. Civ. Eng. 2019 (2019) 1–7.
[11] F. Sayahi, M. Emborg, H. Hedlund, A. Cwirzen, Effect of admixtures on mechanism of plastic shrinkage cracking in self-consolidating concrete, ACI Mater. J. 117 (51–9) (2020), https://doi.org/10.14359/51724623.
[12] S.N. Leonovich, Modelling of Capillary Shrinkage and Cracking in Early-Age Concrete, Sci. Technique 17 (265–77) (2018), https://doi.org/10.21122/2227-1031-2018-17-4-265-277.
[13] P.J. Uno, Plastic Shrinkage Cracking and Evaporation Formulas, 1998.
[14] H.-G. Kwak, S.-J. Ha, Plastic shrinkage cracking in concrete slabs. Part II: numerical experiment and prediction of occurrence, Mag. Concr. Res. 58 (8) (2006) 517–532.
[15] P. Turcry, A. Loukil, Evaluation of plastic shrinkage cracking of self-consolidating concrete, ACI Mater. J. (2006). July-August: 272–9.
[16] R. Combrinck, W.P. Boshoff, Typical plastic shrinkage cracking behaviour of concrete, Mag. Concr. Res. 65 (2013) 486–493, https://doi.org/10.1680/macr.12.00139.
[17] V. Slowik, M. Schmidt, D. Kassler, M. Eiserbeck, Capillary pressure monitoring in plastic concrete for controlling early-age shrinkage cracking, Transp. Res. Rec. 2441 (2014) 1–5, https://doi.org/10.3141/2441-01.
[18] EN 12350-2. EN 12350-2:2019 Testing of fresh concrete. Part 2, Slump-test. Brussels: European Committee for Standardization 2019.
[19] EN 12390-3. EN 12390-3:2000. Testing of hardened concrete. Part 3, Compressive strength of test specimens. Brussels: European Committee for Standardisation 2000.
[20] ASTM C403. ASTM C403:2005. Standard Test Method for Time of Setting of Concrete Mixtures by Penetration Resistance. West Conshohocken: ASTM International 2005.
[21] EN 480-4. EN 480-4:2006. Admixtures for concrete, mortar and grout - Test methods. Part 4, Determination of bleeding of concrete. Brussels: European Committee for Standardisation 2006.
[22] Afrisam. Rapid Hard Cement - AfriSam. <https://www.afrisam.co.za/products-services/cement/rapid-hard-cement>; 2021 [accessed 21.06.21].
[23] Combrinck R. Plastic Shrinkage Cracking in Conventional and Low Volume Fibre Reinforced Concrete. Master's. Stellenbosch University, 2011.
[24] ASTM C 1579. ASTM C 1579: 2006. Standard Test Method for Evaluating Plastic Shrinkage Cracking of Restrained Fiber Reinforced Concrete. West Conshohocken: ASTM International 2006.
[25] R. Combrinck, L. Steyl, W.P. Boshoff, Interaction between settlement and shrinkage cracking in plastic concrete, Constr. Build. Mater. 185 (2018) 1–11, https://doi.org/10.1016/j.conbuildmat.2018.07.028.
[26] D.G. Toll, S.D.N. Lourenço, J. Mendes, in: Advances in suction measurements using high suction tensiometers, 2013, pp. 29–37, https://doi.org/10.1016/j.enggeo.2012.04.013.
[27] P.F. le Roux, S.W. Jacobsz, Performance of the tensiometer method for the determination of soil-water retention curves in various soils, Geotech. Test. J. 44 (2021) 1079–1096, https://doi.org/10.1520/GTJ20200196.
[28] R.C. Deysel, Controlling capillary pressure in concrete to prevent plastic shrinkage cracking, University of Pretoria, Masters, 2022.
[29] E. Holt, M. Leivo, Cracking risks associated with early age shrinkage, Cem. Concr. Compos. 26 (2004) 521–530, https://doi.org/10.1016/S0958-9465(03)00068-4.